DYNAMICS OF A FLUID CONTAINED IN A SPINNING, CONING CYLINDER

Raymond Sedney*
Philip Hall**
Nathan Gerber***
U.S. Army Ballistic Research Laboratory
Aberdeen Proving Ground, Maryland

Abstract

The fluid motion inside a cylinder which simultaneously spins and cones is determined according to linear theory for small coning angles. The Navier-Stokes equations are solved by expansions in spatial eigenfunctions. This form of spectral method gives an efficient solver over a wide range of Reynolds numbers; cases for $Re \leq 2{,}500$ have been computed. The results are validated by comparing computed and measured pressure and moment coefficients. Comparisons are also made with results from a nonlinear finite difference method for which the CPU time is about 400 times that of the present method. The CPU time for the spatial eigenvalue method varies from 10 seconds at Re = 10 to 25 minutes at Re = 1,000. The restriction of linear theory is not severe; for coning angle of 20°, the moment coefficient from linear and nonlinear computations differ by 2%.

I. Introduction

Consider a cylinder of radius a and height 2c which rotates about its axis with a constant angular velocity Ω. The cylinder is filled with an incompressible fluid of density ρ and kinematic viscosity ν. After transient effects (spin-up) have died out, the fluid motion is simply solid body rotation, neglecting gravitational effects. If the cylinder is made to cone at a constant rate τ with respect to an inertial reference frame, the motion is a perturbation on solid body rotation after transient effects have died out. In coning motion, the axis of the cylinder moves on a cone; for convenience, the vertex of the cone is taken to be at the geometrical center of the cylinder. The angle between the cylinder and cone axes is K_0. For small K_0, the Navier-Stokes equations can be linearized. The linearized oscillations of the fluid, forced by the coning, are the subject of this paper. The goal is to predict the pressure on the cylinder walls and the moment which tends to overturn the cylinder, for which experimental data exist.

Although there are applications of the stated problem to the stabilization of certain spacecraft, the motivation here is application to ballistics of liquid-filled projectiles. Such projectiles are often unstable, even though the same projectile with a solid payload is stable. Stewartson[1] showed, for an inviscid fluid, that the mechanism by which the fluid causes the instability is a resonance between the frequency τ and the frequency of inertial waves in the fluid. Subsequent work on the problem, through 1985, is surveyed by Sedney;[2-3] since then, some additional work[4-7] has appeared.

Previous work on the problem has employed the inertial reference frame, S, used here, or an aeroballistic reference frame, S', with one axis coincident with the cylinder axis. In S', the boundary conditions are easier to apply. The solution for the fluid motion depends on three nondimensional parameters: Reynolds number = Re, frequency = f, and aspect ratio = A = c/a. Since the cylinder angular velocity in S is $\Omega + \tau \cos K_0$, it is appropriate to define

$$Re = (\Omega + \tau \cos K_0)\, a^2/\nu$$
$$f = \tau/(\Omega + \tau \cos K_0). \qquad (1)$$

For reference, these are, in S',

$$Re' = \Omega\, a^2/\nu$$
$$f' = \tau/\Omega.$$

For the linearized problem, $\cos K_0 = 1$. Time, length, velocity, and pressure are made nondimensional by $(\Omega + \tau)^{-1}$, a, $(\Omega + \tau)a$, and $\rho a^2(\Omega + \tau)^2$, respectively.

Details of the process of arriving at the linear partial differential equations and boundary conditions are given in Reference 8; only an outline is given here:

a. The Navier-Stokes equations are written in cylindrical polar coordinates (r,θ,x) in S with corresponding velocity components (u,v,w).

b. The boundary conditions on the cylinder wall are determined from the projectile motion which is proportional to exp $i(ft-\theta)$ where t is time.

c. For linear perturbation on solid body rotation, the velocity components are written $(-K_0u^*,\ r-K_0v^*,\ -K_0w^*)$ and pressure as $1/2\ r^2 - K_0p^*$. The * denotes perturbation.

d. It is convenient to introduce complex velocities and pressure, denoted by sub _ and defined by

$$(u^*,v^*,w^*,p^*) = \text{Real}\left\{(\underline{u},\underline{v},\underline{w},\underline{p})\ \exp\ i(ft-m\theta)\right\} \qquad (2)$$

where the azimuthal wave number, m, is an integer $(\pm)$ but only m = 1 is needed for the linear forced motion problem.

The resulting linearized, non-dimensional Navier-Stokes equations are:

---

*Research Scientist, Launch and Flight Division
Associate Member AIAA
**Department of Mathematics, Exeter University, Exeter, England; ICASE, Hampton, Virginia
***Aerospace Engineer, Launch and Flight Division
Member AIAA

$$i(f-1)\,\underline{u} - 2\underline{v} = -\underline{p}_r + Re^{-1}\left[\nabla^2\underline{u} - \frac{2}{r^2}\underline{u} + \frac{2i}{r^2}\underline{v}\right]$$

$$i\,(f-1)\underline{v} + 2\underline{u} = (i/r)\underline{p} + Re^{-1}\left[\nabla^2\underline{v} - \frac{2}{r^2}\underline{v} - \frac{2i}{r^2}\underline{u}\right]$$

$$i\,(f-1)\,\underline{w} = -\underline{p}_x + Re^{-1}\left[\nabla^2\underline{w} - \frac{1}{r^2}\underline{w}\right]$$

$$(r\underline{u})_r - i\,\underline{v} + r\underline{w}_x = 0\ , \qquad (3)$$

where $\nabla^2 = \partial_r{}^2 + (1/r)\,\partial_r + \partial_x{}^2$ is the Laplacian and subscripts denote partial derivatives.

From Eq. (3) and boundary conditions, the eigenvalue and forced motion problems are defined. Particular solutions which simplify application of boundary conditions are found. The solution is expressed as an eigenfunction expansion; therefore, it is in the class of spectral methods. The spatial eigenvalue expansion approach was used by Blennerhasset and Hall[9] and Hall[10] in their investigations of the Taylor vortex problem for finite length cylinders. In that problem and the present one, the complex eigenvalues separate into triplets; the existence of three groups of modes must be reckoned with to obtain accurate numerical solutions.

The coefficients in the expansion are determined by satisfying boundary conditions. Then, the velocity components and pressure are known so that pressure and moment coefficients can be calculated. Numerically, there are two issues: calculation of the eigenvalues and determination of the expansion coefficients. Using asymptotic estimates, extrapolation, and interpolation the first of these is well in hand. The coefficients in the expansions have been determined by collocation and a least squares method. For Re < 200, the results from the two methods agree to 1% or less. For some cases with Re > 200, the difference is 5% in the moment coefficient and 1% in pressure coefficient; for these, cancellation among the four contributions to the moment apparently causes the difference.

The spatial eigenvalue method is applied here to the linear problem (extension to the nonlinear case is underway). Thus, K_0 must be small in some sense; comparing the present results with those from finite difference methods (nonlinear) for K_0 = 20° indicated that the nonlinear effect is not large. The spatial eigenvalue method can be applied to any Re, in principle; so far calculations have been made for Re $\lesssim$ 2,415. Since more data is available for Re < 200, greater consideration is given to that range in the presentation of results.

In general, CPU time on the VAX 8600 is of the order of minutes, increasing with Re; for Re = 10, f = 0.05 and, aspect ratio = 3.0, it is 10 seconds if 6 eigenvalues are used (with a maximum of 4 iterations) and 30 seconds if 15 eigenvalues are used (with a maximum of 8 iterations). The side moment coefficients computed with 6 or 15 eigenvalues differ by 0.15% for this case. For Re =1,000 and f = 0.1, the CPU time is approximately 25 minutes. A technique which reduces CPU time has been tested in a few cases, giving a reduction of 1/3.

II. Statement of the Problem

As for any oscillatory system two problems are defined: the free oscillation or eigenvalue problem and the forced oscillation problem here called the moment problem. For the eigenvalue problem, the complex perturbation velocities and pressure in Eq. (2) are written

$$(\underline{u},\underline{v},\underline{w},\underline{p}) = \big(U(r)\sin Kx,\ V(r)\sin Kx,\ W(r)\cos Kx,\ P(r)\sin Kx\big).$$

From Eq. (3) the radial variations (U,V,W,P) satisfy

$$\left[Re^{-1}(\Delta_1 - r^{-2}) - iM\right]U + 2\left[1+(i/r^2\,Re)\right]V - P_r = 0$$

$$\left[Re^{-1}(\Delta_1 - r^{-2}) - iM\right]V - 2\left[1+(i/r^2\,Re)\right]U + \frac{iP}{r} = 0$$

$$\left[Re^{-1}\,\Delta_1 - iM\right]W - KP = 0$$

$$(rU)_r - iV - KrW = 0\ , \qquad (4)$$

where $M = f - 1$,

and $\Delta_1 \equiv \partial_{rr} + \frac{1}{r}\partial_r - \left[\frac{1}{r^2} + K^2\right]$.

The boundary conditions are

$$U = V = W = 0 \qquad \text{at } r = 1, \qquad (5)$$

the no-slip condition, and

$$U - iV = W = P = 0 \quad \text{at } r = 0.$$

Discussions of the origin of these boundary conditions are given in References 8 and 11. Equations (4) and (5) constitute an eigenvalue problem for $K = K(m,Re,f)$. Since the problem is defined on a finite interval, it is expected that the spectrum will be infinite and discrete. If neutral disturbances were possible, then K would, of course, be real; in this problem, the K are complex. The numerical solution of the eigenvalue problem is discussed in the next section; here it is assumed that an infinite sequence of eigenvalues exists.

For the moment problem, the boundary conditions at r = 1 and x = ±A are

$$\underline{u} = -i\,(1 - f)\,x$$

$$\underline{v} = -(1 - f)\,x \qquad (6)$$

$$\underline{w} = i\,(1 - f)\,r\ ,$$

see Reference 8. It is convenient to transfer the inhomogeneous boundary conditions to the endwalls by subtracting out a suitable particular solution to the perturbed Navier-Stokes equations. Let

$$\underline{u} = -i\,[1 - f]\,x + u\,(r,x)$$

$$\underline{v} = -[1 - f]\,x + v\,(r,x)$$

$$\underline{w} = i\,[1 - f]\,r + \sigma(r) + w\,(r,x) \qquad (7)$$

$$\underline{p} = -[1 - f^2]\,rx + p\,(r,x)$$

$$\sigma(r) = 2if\left[r - \frac{J_1(\lambda r)}{J_1(\lambda)}\right]$$

where J_1 is the Bessel function of the first kind and order 1 and $\lambda = (1 + i)\,[(1 - f)\,Re/2]^{1/2}$. By construction (u,v,w,p), satisfy Eq. (3); the boundary conditions are

$$u - iv = w = p = 0, \qquad r = 0 \qquad (8a)$$

$$u = v = w = 0, \qquad r = 1 \qquad (8b)$$

$$u = v = 0,\ w = -\sigma(r) \qquad x = \pm A \qquad (8c)$$

Assuming that $(u,v,p) = (U(r), V(r), P(r))\sin Kx$ and $w = W(r)\cos Kx$, it follows that U,V,W,P satisfy Eq. (4); the odd and even variations with x follow from Eqs. (6) and (7). Let the infinite sequence of eigenvalues be denoted by $\{k_n\}$ and the eigenfunctions by u_n, v_n, w_n, p_n. The solution is expressed as an eigenfunction expansion:

$$(u,v,w,p) = \sum_{n=1}^{\infty} (\alpha_n \sin k_n x/\sin k_n A)\times (u_n, v_n, w_n \cot k_n x, p_n) \qquad (9)$$

The solution, Eq. (9), satisfies Eqs. (8a,b); the endwall boundary conditions, Eq. (8c), are used to find the undetermined coefficients α_n.

III. Calculation of the Eigenvalues and Coefficients

Two independent methods were used to compute the eigenvalues; since both iterative methods are well documented elsewhere, only a brief description of them is given. Firstly, the complete orthonormalization procedure of Davey,[12] as implemented by Kitchens, Gerber, and Sedney[13] was employed. The numerical integration was carried out using a fourth order Runge-Kutta scheme. Secondly, the compact finite difference scheme of Malik, Chuang, and Houssaini[14] was used. In both methods the singularity in the equations at $r = 0$ was removed by transferring the numerical integration boundary to $r = \varepsilon$, with $0 < \varepsilon << 1$, and using the Taylor series solution given in Reference 13 to evaluate the dependent variables at $r = \varepsilon$. The methods gave consistent results.

With both methods, a sufficiently accurate guess for k_n was required if the iterations were to converge. This was a hindrance initially since little previous knowledge of the distribution of these eigenvalues was available; in certain cases it was necessary to calculate a large number of the sequence $\{k_n\}$. To obtain first guesses, techniques were developed to determine approximations to the eigenvalue distribution in certain special limits, and if necessary, follow their evolution into the required regime.

A Related Taylor Vortex Problem.

Firstly, previous knowledge of the eigenvalue distribution for the classical Taylor vortex problem was used.[9] Consider a basic flow driven by the rotation of the cylinder $r = \varepsilon$ while the outer cylinder is held fixed. No-slip boundary conditions are applied at $r = \varepsilon$ and at $r = 1$. The frequency, f, and azimuthal wave numbers, m, are now set to zero. There are three sets of eigenvalues: (1) a pure imaginary set $\{k_{3n}\}$, (2) a complex set $\{k_{3n+2}\}$, with $k_{3n+2} = \bar{k}_{3n+1}$, (3) a complex set k_{3n+1}, in the first quadrant with real part $\sim \pi$; $n = 1,2,\ldots$. Blennerhasset and Hall[9] found that the eigenvalues $\{k_{3n}, k_{3n+1}, k_{3n+2}\}$ have azimuthal velocity eigenfunctions with n zeros in $(\varepsilon,1)$. Thus, in the axisymmetric problem, there is a rational method of ordering the eigenvalues, in triplets. If m or f is now taken to be nonzero, the symmetry of the eigenvalue distribution described above is broken but the ordering from the axisymmetric steady Taylor vortex problem can be retained. The parameters are gradually changed to those of the present problem and the eigenvalues determined numerically. Details of this method are given in Reference 7. It was efficient for $Re < 100$. Another approach, for small Re, which gives first guesses for an arbitrary number of eigenvalues, is described next.

Re → 0.

For values of $Re \lesssim 10$, approximately, estimates for the eigenvalues can be found by solving the $Re \to 0$ problem, i.e., the Stokes limit. Essentially, the same procedure is used as for the classical Stokes flow solution, but $Re \to 0$ is a regular perturbation for the internal flow under consideration. Details are described in Reference 7.

The eigenfunctions, $\lim_{Re\to 0} (u_n, v_n, w_n, p_n)$, can be found explicitly in terms of the Bessel functions J_0, J_1, and J_2. The eigenvalues, $\lim_{Re\to 0} k_n$ are the zeros of a transcendental equation involving the same Bessel functions and do not depend on any of the parameters of the problems; these zeros are found using a standard routine. The first several eigenvalues, in this limit, are shown in Figure 1. They separate into three branches on which the eigenvalues are: (1) pure imaginary, (2) in the 4th quadrant, and (3) conjugate to (2). This is the same separation noted above in the Taylor vortex problem; the bases for that problem and the Stokes limit are completely different, of course.

To indicate this separation, an alternate notation for the eigenvalues, $k_{\ell,n}$, is introduced where $\ell = 1,2,3$ denotes the branch and $n = 1,2,\ldots$ is the index along a branch. For $n >> 1$ and using the asymptotic properties of the Bessel functions, $\lim_{Re\to 0} \mathrm{Im}\,(k_{\ell,n+1} - k_{\ell,n}) \approx \pm\,\pi$, with + for $\ell = 1,3$,

and - for $\ell = 2$. Empirically, it was found that the eigenvalues for finite Re satisfy the same relation if $n > n_0(Re)$; the function $n_0(Re)$ is only known empirically. Given $k_{\ell,n}$ for $1 < n < n_0$, using this relation for the imaginary part and extrapolation for the real part provide an effective algorithm for estimating $k_{\ell,n}$, $n \geq n_0$.

Starting from $\lim_{Re \to 0} k_{\ell,n}$, extrapolating in Re and/or f and using the algorithm, the eigenvalues for any Re and f can be estimated. Relatively large increments in Re can be used for $\ell = 1$ (in general, it is easier to estimate $k_{1,n}$) but smaller for $\ell = 2,3$. Using a systematic extrapolation process, Mermagen[15] constructed a table of $k_{\ell,n}$ for $0 \leq f \leq 1$ and $0 \leq Re \leq 2{,}500$; the estimates were processed through one of the eigenvalue solvers described above so that no further use of the solver is necessary. This is the basis for reducing CPU time mentioned above.

Results for Re = 100, f = 0.1 and $n \leq 5$ are shown in Figure 1. The first eigenvalue on each branch and $k_{3,2}$ are labeled. Note the separation of $k_{3,2}$ and $k_{3,1}$. The ordering of the $k_{\ell,n}$ is determined by the number of zeros of the eigenfunctions: n zeros corresponding to $k_{1,n}$ and n - 1 zeros corresponding to $k_{2,n}$ or $k_{3,n}$.

In calculating the flow variables, the ordering of the $k_{\ell,n}$ must be preserved; they are taken in groups of three: $\ell = 1,2,3$ for $n = 1$, $n = 2$, etc. Departure from this ordering introduces errors; the error depends mainly on the degree of departure, n, and on the method used to calculate α_n.

A more efficient method of estimating $k_{\ell,n}$, especially $k_{2,n}$ and $k_{3,n}$, for large Re was needed and for this purpose asymptotic approximations were derived.

Re → ∞.

Asymptotic approximations were derived first by assuming $k \sim \tilde{\kappa}_0 + \tilde{\kappa}_1 Re^{-1/2}$ for branch 1 and $k \sim \kappa_0 Re^{1/2} + \kappa_1 Re^{-1/2}$ for branches 2 and 3 with appropriate expansions for the flow variables. Although a boundary layer exists at r = 1, it does not enter the calculation of the first two terms for k. The results of the anaysis gave suitable first guesses for small n, e.g., n = 5 for Re = 1000, f = 0.1; see Reference 7. An alternative approach based on the WKB method was derived which gave suitable first guesses for, essentially, all eigenvalues. The solution is in the form of a triple deck with boundary layers of thickness $O(Re^{-1/2})$ at r = 0 and r = 1 plus the core region for $0 < r < 1$. The eigenfunctions in the boundary layer at r = 0 are $Re^{1/4}$ larger than in the core. In the analysis, the mode number, n, is formally $O(Re^{1/2})$; in practice $n \geq 1$ was used. For example, this method gave first guesses which converged to the eigenvalues $k_{\ell,n}$ for Re = 1,000, f = 0.1, and $n \geq 1$. However, for Re = 2415 and f = 0.1 the WKB results converged for $n > 3$; for $n \leq 3$, the first mentioned asymptotic method gives the required results. The versatility of the method is shown by the fact that it provides accurate first guesses for $Re \geq 1$ and $n \geq 1$; thereby, overlapping the method for Re → 0. Thus, numerical approaches described in this section provide the means to determine the eigenvalues.

Calculation of the Coefficients α_n

Reverting to the first notation for the eigenvalues, assume that $\{k_n\}$ are known for $1 \leq n \leq 3M$, where M is a positive integer. Truncating the series in Eq. (9) at n = 3M, the coefficients $\{\alpha_n\}$, $1 \leq n \leq 3M$, were determined by either of two ways. The first is collocation. Let $\{r_j\}$, $1 \leq j \leq M$, be a sequence of points such that

$$\varepsilon < r_1 < r_2 \ldots < r_M < 1.$$

Enforcing the boundary conditions Eq. (8) at the points $r_1, \ldots, r_M$ leads to

$$\begin{aligned} E_1(r_j) &\equiv \sum_{n=1}^{3M} \alpha_n u_n(r_j) = 0 \\ E_2(r_j) &\equiv \sum_{n=1}^{3M} \alpha_n v_n(r_j) = 0 \\ E_3(r_j) &\equiv \sum_{n=1}^{3M} (\alpha_n \cot k_n A) w_n(r_j) + \sigma(r_j) = 0 . \end{aligned} \tag{10}$$

These 3M linear equations are solved for the coefficients $\alpha_1, \ldots \alpha_{3M}$. The success of the method requires that the flow properties converge in some sense as M increases. Experience has shown, for $Re \leq 1{,}000$, that the required value of M to achieve a given accuracy increased monotonically with Re. Numerical examples are given in Section V.

The second is a least squares method. The "normal" equations for α_n are obtained by minimizing the error

$$g(\alpha_n) = \int_0^1 \left\{ |E_1(r)|^2 + |E_2(r)|^2 + |E_3(r)|^2 \right\} r^e \, dr . \tag{11}$$

Exponents e = 0,1 gave essentially the same results. A measure of the error, E, in α_n is given by

$$E^2 = g \Big/ \int_0^1 |\sigma(r)|^2 \, r^e \, dr, \tag{12}$$

which is applicable to both methods. Individual measures of error for u, v, and w are defined similarly. They relate to the satisfaction of the endwall boundary conditions only and, therefore, not to derivatives of u, v, and w which are required in the calculation of the moment. However, they have been useful in evaluating the efficacy of the methods. A discussion of the two methods is given later.

IV. Pressure and Moment Coefficients

Having the velocity and pressure from the spatial eigenvalue method, pressure and moment coefficients can be computed and compared with measurements of these quantities. The moment coefficient is used in the study of projectile stability. Only the pressure coefficient on the endwall is considered here. In experiments pressure transducer measurements[4] are processed to produce amplitude and phase; the amplitude is proportional to the pressure coefficient, C_p, defined here.

$$C_p = [(p_R + f^2 rx)^2 + p_I^2]^{1/2}, \qquad (13)$$

where sub R and I denote real and imaginary parts of p, respectively; Eq. (13) is derived in Reference 7. Since the spatial eigenvalue method is semi-analytical, useful limiting forms of C_p can be derived, as given in Reference 7. An exact result, even for the nonlinear case, is $C_p = rx$ for $f = 1$.

Of the three components of the moment, the axial or roll component is zero to $O(K_o)$ and the transverse components are $O(K_o)$. The transverse components can be separated into the overturning or side moment and the in-plane moment which acts to change the coning rate.[16] The side moment is important for projectile stability, as shown by Murphy,[16] and is the only component considered. The following definition[16] is used: nondimensional side moment coefficient $\equiv C_{LSM}$ = side moment/ $2\pi\rho a^4 c (\bar{\tau} + \Omega)^2 f K_o$; C_{LSM} is expressed as the sum of the four contributions: (a) the pressure on the sidewall, (b) pressure on the endwalls, (c) shear force on the sidewall, and (d) shear force on the endwalls, given by

$$\text{(a)}\quad (fA)^{-1} \int_0^A x\, \underline{p}_I\,(1,x)\, dx$$

$$\text{(b)}\quad -(fA)^{-1} \int_0^1 \underline{p}_I\,(r,A)\, r^2\, dr \qquad (14)$$

$$\text{(c)}\quad -(fARe)^{-1} \int_0^A \left[\partial\,(x\underline{v}_R - \underline{w}_I)/\partial r \,\Big|_{r=1} + 1 - f\right] dx$$

$$\text{(d)}\quad -(f\,Re)^{-1}\, \text{Real}\left[1-f + \int_0^1 \partial\,(\underline{v} - i\underline{u})/\partial x \,\Big|_{x=A}\, r\, dr\right],$$

respectively. The presence of derivatives in (c) and (d) indicate, possibly, a greater error than in the evaluation of C_p. Note that $C_{LSM} = 0$ for $f = 1$.

V. Numerical Aspects

Methods for determining the first guesses for the eigenvalues have been described. To calculate the converged eigenvalues and eigenfunctions, by either the finite difference or orthonormalization technique, the number of integration points must be chosen which must be related to the number of zeros of the eigenfunctions. For given M, the largest number of zeros is M, for the (1,M) mode. A number of points in $\varepsilon \le r < 1$ equal to 7M was found to be adequate although a larger number was usually employed. Other numerical parameters having to do with the number of terms in series, convergence of iteration processes, etc, will not be discussed.

The central numerical parameter is the number of eigenvalues, N = 3M, the choice of which is more sensitive to Re than f or A; recall that the $k_{\ell,n}$ are independent of A. Accurate determination of the α_n, and therefore, the solution (u,v,w,p), depends mainly on N. Experience has shown, for $Re \le 1{,}000$, that the required value of N, to achieve a given accuracy, increased monotonically with Re. For example, N = 6 is sufficient for Re = 1; whereas, N = 60 was required for Re = 1,000; the rate of increase is smaller for Re > 1,000. An obvious requirement is that the solution "converges" for increasing N, i.e., the solution is sensibly independent of N. Convergence depends, to some extent, on the method used to determine α_n.

Collocation and least squares methods were used to solve for α_n; the corresponding programs are denoted by COL and LS, respectively. In LS, the only choice to be made is the number of integration points in Eq. (11), which is not critical. In COL the distribution of the M collocation points, which can be critical to the success of the calculation, must be chosen. Equal spacing of the collocation points (exactly or to within ±1 of the point number) was found to be optimum, empirically. Some support for this is indicated by the fact that the M zeros of the (1,M) eigenfunctions are essentially equally spaced for $M \ge 10$; the core solution in the WKB method also gives equal spacing. Since the function $\sigma(r)$ exhibits a boundary layer type behavior near r = 1 for $Re \approx 1{,}000$, concentration of collocation points near r = 1 would seem to be advisable; in fact this had a deleterious effect on the solution.

According to the formulation of the problem, there is a discontinuity in u and v at the points $x = \pm A$, $r = 0$. The endwall boundary conditions, Eq. (8), require $u = v = 0$ for $0 < r < 1$. On the other hand, the boundary conditions on the eigenfunctions, Eq. (5), require $u_n - iv_n = 0$ at $r = 0$ so that, from Eq. (9), $u - iv = 0$; but u and v are not separately zero at r = 0. The presence of this discontinuity had a negligible effect on the solution for $Re < 200$ but not for larger Re. For the determination of α_n the discontinuity was removed by requiring that $u + iv = 0$ at $r = \varepsilon$, the smallest r that can be used in determining α_n.

In COL the condition $u + iv = 0$ at $r = \varepsilon$ is used as an additional collocation equation with another eigenvalue, (1,M+1), included. An illustration of the effect of removing the discontinuity is shown in Figure 2, using COL. The "error" $E_1(r)$, see Eq. (10), is plotted vs r with the discontinuity present or not. Removing the discontinuity gives a large reduction in E_1 near $r = \varepsilon$; a significant reduction is also obtained near $r = 1$. The effect on C_p is relatively small, but on C_{LSM} it is significant.

A comparison of the calculation of C_{LSM} by LS and COL is shown in Figure 3 for $3 \leq N \leq 42$ with $Re = 21.5$, $f = 0.0621$, and $A = 1.042$. (A comparison with experimental results for these parameters is given later.) The LS results are less sensitive to decreasing N than the COL results. For $N = 6$, the LS result is within 1.7% of that for large N. The two methods give essentially the same C_{LSM} for $N \geq 12$. The difference for $N = 42$ is 10^{-4} which is representative of the accuracy of the calculation.

The C_p at $r = 0.667$ vs N, using LS and COL, are shown in Figure 4 with $Re = 1{,}000$, $f = 0.1$, and $A = 3$. The two values differ by 1% at most for $N \geq 48$. The "converged" or limiting value is $C_p\ (0.667) = 0.205$. For $N = 12$, the COL value is 2.4% below the limiting value and the LS value, offscale, is 7.8% below.

For $Re \leq 200$, limiting values from LS and COL were essentially the same. For $Re > 200$ and small C_{LSM}, $C_{LSM} \approx 0.02$, they disagreed by approximately 0.005 in the values of C_{LSM}. For small C_{LSM} cancellation of the terms in Eq. (14) make accurate calculation more difficult. For $Re > 200$ the pressure contributions to C_{LSM} (14a,b) begin to dominate the shear contributions (14c,d) as expected.

VI. Results

In the following N was chosen large enough to give the limiting values of C_p and C_{LSM}. When quoting results from finite difference methods or experiments, for comparisons, K_0 must be specified; results from the linear theory used here are independent of K_0, of course. In projectile applications $1 \leq Re < 10^6$, $0 < f < 0.2$, $1 < A < 5$; in laboratory experiments, measurements for $-0.5 \leq f \leq 1.1$ have been made of C_p and of C_{LSM}.

A comparison of calculated pressure coefficient vs f with some experimental measurements of Hepner, Kendall, Davis, and Tenly[4] is shown in Figure 5 for $Re = 3.1$ and $A = 3.148$. The pressure transducer was located at $r = 0.667$ and the coning angle was $K_0 = 2°$. The radius of the cylinder was 3.18 cm; the fluid had a density of 0.969 gm/cm^3 and a kinematic viscosity of 60,000 cs. The data include estimates of errors in C_p, as presented by Hepner et al.[4] For almost all points, the calculated C_p is less than the measured C_p; for the larger f it is outside the error bar. The reason for the bias in this comparison is not known.

Comparison of results from the spatial eigenvalue method and finite difference methods is the most obvious. The first finite difference solution for this problem was presented by Vaughn, Oberkampf, and Wolfe[17] using dimensional quantities throughout. Nusca and D'Amico[6] report a dimensional inhomogeneity in the work of Reference 17 making it impossible to compare with the dimensionless form of the theory presented here. Strikwerda[18] solves the nonlinear Navier-Stokes equations, so that K_0 is arbitrary. Several comparisons of results from the finite difference method of Strikwerda, as computed by Nusca,[19] and the present method are given in Reference 7; one of these is shown in Figure 6 for $0 \leq Re \leq 1$, $f = 0.1$, $A = 3.0$, $K_0 = 2°$. The maximum difference in C_{LSM} is 0.3×10^{-4} at $Re = 1.0$.

The variation of C_{LSM} with f is given in Figure 7 over the range of $0 \leq f \leq 1.1$ for the spatial eigenvalue calculations and $0.05 \leq f \leq 0.9$ for the Strikwerda results, $K_0 = 2°$, both for $Re = 10.0$ and $A = 3.0$. The two sets of results are essentially the same, which tends to support the validity of each. The maximum difference is .0025 at $f = 0.6$. The existence of a maximum in this curve is of some interest. When the first measurements of C_{LSM}, from yaw growth rate, were made at "small" Re, a linear variation of C_{LSM} with f was found, but only over the range $0 < f < 0.15$. It was speculated that for "small" Re a Stewartson resonance[1] does not occur. Figure 7 shows that resonance does occur at $Re = 10$, albeit, highly damped. Of course, Stewartson's theory was formulated for an inviscid fluid and its extensions apply to "large" Re so that quantitative results from these could not be expected to apply at $Re = 10$.

A comparison of calculated side moment coefficients vs f with experimental measurements of D'Amico[20] is shown in Figure 8 for $Re = 21.5$, $A = 1.042$ and $Re = 133$, $A = 1.486$, both for $K_0 = 2°$. The experimental results were deduced from yaw growth rate measurements on a gyroscope. The calculated C_{LSM} is linear for $0 \leq f \leq 0.035$, approximately. For $Re = 21.5$, the experimental and calculated results agree for the two larger values of f. The reason for the discrepancy at $f = 0.045$ is not known; although, it is pointed out in Reference 20 that, as C_{LSM} decreases, the error in its measurement increases; no error bounds were presented. For $Re = 133$ the data are uniformly below the calculated results. If extrapolated, the trend of the data implies $C_{LSM} = 0$ for $f = 0.03$, approximately and negative values for $f < 0.03$. In all cases computed thus far, C_{LSM} is positive for $0 < f < 1$.

A new result, which has possible practical application, was found from the spatial eigenvalue calculations. For $Re = 1{,}000$ and $f = 0.1$, a resonance behavior was found of C_p and C_{LSM} with

varying A for A ≈ 1.0. Usually, resonant response tuned by f is investigated in this problem. Results shown in Reference 7 are qualitatively correct but were obtained with the discontinuity present; calculations without the discontinuity will be reported later.

Calculated values of C_{LSM} vs f are shown in Figure 9 together with experimental measurements of D'Amico (unpublished) for Re = 2415 and A = 1.042. In these calculations, the discontinuity was removed. Over the range of f for which data was obtained, C_{LSM} decreases monotonically with f. The calculated C_{LSM}, for $0.04 \leq f \leq 0.08$, have a maximum at f = 0.055. The maximum difference between the data and calculations is 2.7% at f = 0.055. The theory of Reference 8, which is asymptotic for Re → ∞, gives C_{LSM} which are about 10% below the present calculations and the data in the neighborhood of f = 0.06 indicating that it is applicable only for Re > 2415 at least for A = 1.042.

An attempt was made to compare the moment coefficients calculated by this linear theory to those obtained from the large scale numerical methods in which linearity in K_0 is not assumed. In addition to the finite difference method of Reference 18, a finite element method was recently applied to this problem by Rosenblat[21] from which a limited number of results is available. Results for moment coefficient, with K_0 = 20°, are presented in Table 1 from these methods and the spatial eigenvalue method. The comparison was frustrated because the results using the methods of References 18 and 21 differ significantly, as seen in Table 1. Therefore, a definitive statement on the effects of departure from linearity at K_0 = 20° cannot be made. In Table 1 Reynolds number, frequency and moment coefficient are given in the aeroballistic reference frame, S', used in References 18 and 21, and denoted by Re', τ', and C_{LSM}'. The comparisons are made in S' because fewer calculations were required.

TABLE 1. Comparison of C_{LSM}' by the Spatial Eigenvalue, Finite Difference and Finite Element Methods; τ' = 0.1670, A = 4.29, K_0 = 20°.

	C_{LSM}'		
Re'	Ref. 18,19	Reference 21	Spatial E.V.
5.90	0.03172	0.03082	0.03104
11.42	0.04732	0.04378	0.04785

The differences between the spatial eigenvalue results and those of Reference 21 are 0.7% and 10% for Re' = 5.90 and 11.42, respectively. Between the spatial eigenvalue results and those of Reference 18, the corresponding differences are 2.2% and 1.1% which are no greater than the differences between these methods for K_0 = 2°. Although a wider range of parameters must be investigated to arrive at a definitive conclusion, it appears that the nonlinear effect is small up to K_0 = 20°.

VII. Discussion

It has been demonstrated that the linearized Navier-Stokes equations with boundary conditions appropriate to a spinning, coning cylinder can be solved by eigenfunction expansions over a wide range of the governing nondimensional parameters: Re, f, and A. By expanding the complete solution in powers of a small parameter related to coning angle, the nonlinear problem can also be solved by eigenfunction expansions. The restriction of this linear theory to small coning angle does not appear to be a severe one, based on available results from finite difference/element methods.

The method described here is versatile and requires relatively little CPU time. It has been validated by comparisons with results from large scale finite difference/element methods and with experimental data. Some improvements in the method are contemplated, especially in the determination of the coefficients in the eigenfunction series.

REFERENCES

1. Stewartson, K., "On the Stability of a Spinning Top Containing a Liquid," J. Fluid Mech., Vol. 5, Part 4, September 1959, pp. 577-592.
2. Sedney, R., "A Survey of the Fluid Dynamic Aspects of Liquid-Filled Projectiles," AIAA Paper AIAA-85-1822-CP, AIAA 12th Atmospheric Flight Mechanics Conference, Snowmass, CO., August 1985.
3. Sedney, R., "Some Rotating Fluid Problems in Ballistics," article in Mathematics Applied to Fluid Mechanics and Stability: Proceedings of a Conference Dedicated to Richard C. DiPrima, SIAM, pp. 87-109, Philadelphia, PA., 1986.
4. Hepner, D.J., Kendall, T.M., Davis, B.S., and Tenly, W.Y., "Pressure Measurements in a Liquid-Filled Cylinder Using a Three-Degree-of-Freedom Flight Simulator," BRL-MR-3560, U.S. Army Ballistic Research Laboratory, Aberdeen Proving Ground, Maryland, December 1986.
5. Herbert, T. and Li, R., "Numerical Study of the Flow in a Spinning and Nutating Cylinder," AIAA Paper AIAA-87-1445, AIAA 19th Fluid Dynamics, Plasma Dynamics and Lasers Conference, Honolulu, Hawaii, June 1987.
6. Nusca, M.J. and D'Amico, W.P., "Parametric Study of Low Reynolds Number Precessing/Spinning Incompressible Flows," U.S. Army Ballistic Research Laboratory, Aberdeen Proving Ground, Maryland, BRL Memorandum Report in publication.
7. Hall, P., Sedney, R., and Gerber, N., "Fluid Motion in a Spinning, Coning Cylinder via Spatial Eigenfunction Expansion," ARBRL-TR-2813, U.S. Army Ballistic Research Laboratory, Aberdeen Proving Ground, Maryland, August 1987.
8. Gerber, N., Sedney, R., and Bartos, J.M., "Pressure Moment on a Liquid-Filled Projectile: Solid Body Rotation," ARBRL-TR-02422, U.S. Army Ballistic Research Laboratory, Aberdeen Proving Ground, Maryland, October 1982. (AD A120567)
9. Blennerhasset, P.J., and Hall, P., "Centrifugal Instabilities of Circumferential Flow in Finite Cylinders: Linear Theory," Proc. Roy. Soc. London, A-365, pp. 191-207, 1979.

10. Hall, P., "Centrifugal Instabilities of Circumferential Flows in Finite Cylinders: Nonlinear Theories," Proc. Roy. Soc., Series A, Vol. 372, pp. 317-356, 1980.
11. Batchelor, G.K., and Gill, A.E., "Analysis of the Stability of Axisymmetric Jets," Journal of Fluid Mechanics, 14, pp. 529-551, 1962.
12. Davey, A., "A Simple Numerical Method for Solving Orr-Sommerfeld Problems," Quarterly Journal of Mathematics and Applied Mechanics, Vol. 26, Part 4, pp. 401-411, 1973.
13. Kitchens, Jr., C.W., Gerber, N., and Sedney R., "Oscillations of a Liquid in a Rotating Cylinder: Part I. Solid Body Rotation," ARBRL-TR-02081, U.S. Army Ballistic Research Laboratory, Aberdeen Proving Ground, Maryland, June 1978. (AD A057759)
14. Malik, M.R., Chuang, S., and Hussaini, M.Y., "Accurate Numerical Solution of Compressible, Linear Stability Equations," Journal of Applied Mathematics and Physics (ZAMP), Vol. 33, pp. 189-201, March 1982.
15. Mermagen, William H., Private Communication, U.S. Army Ballistic Research Laboratory, Aberdeen Proving Ground, Maryland.
16. Murphy, C.H., "Angular Motion of a Spinning Projectile with a Viscous Liquid Payload," ARBRL-MR-03194, August 1982. (AD A118676). Also Journal of Guidance, Control, and Dynamics, Vol. 6, pp. 280-286, July-August 1983.
17. Vaughn, H.R., Oberkampf, W., and Wolfe, W.R., "Fluid Motion Inside a Spinning Nutating Cylinder," Journal of Fluid Mechanics, Vol. 150, pp. 121-138, 1985. Also "Numerical Solution for a Spinning, Nutating Fluid-Filled Cylinder," Sandia Report SAND 83-1789, December 1983.
18. Strikwerda, J.C., and Nagel, Y.M., "A Numerical Method for Computing the Flow in Rotating and Coning Fluid-Filled Cylinders," CRDC-SP-85006, 1984 Conference on Chemical Defense Research, Aberdeen Proving Ground, Maryland, November 1984.
19. Nusca, M.J., Private communication, U.S. Army Ballistic Research Laboratory, Aberdeen Proving Ground, Maryland.
20. D'Amico, W.P., "Instabilities of a Gyroscope Produced by Rapidly Rotating, Highly Viscous Liquids," AIAA Paper 81-0224, January 1981. Also, Journal of Guidance, Control, and Dynamics, Vol. 7, No. 4, pp. 443-449, July-August 1984.
21. Rosenblat, S., Private Communication, Fluid Dynamics International.

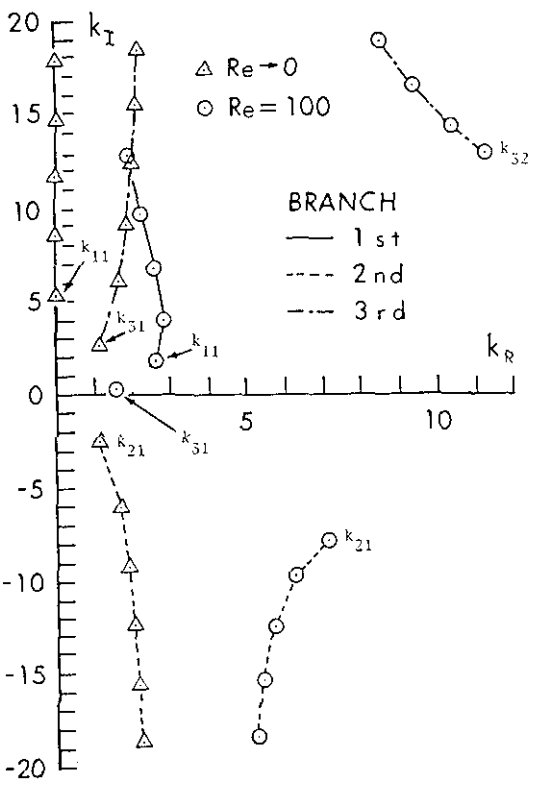

Fig. 1. The first 15 eigenvalues for the Stokes limit and for Re = 100, f = 0.1.

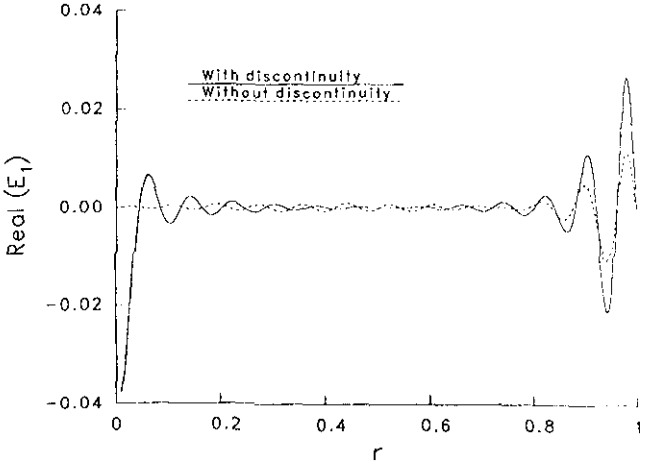

Fig. 2. Real part of the error $E_1(r)$ in the radial velocity u with and without discontinuity at $x \pm A$, $r = 0$.

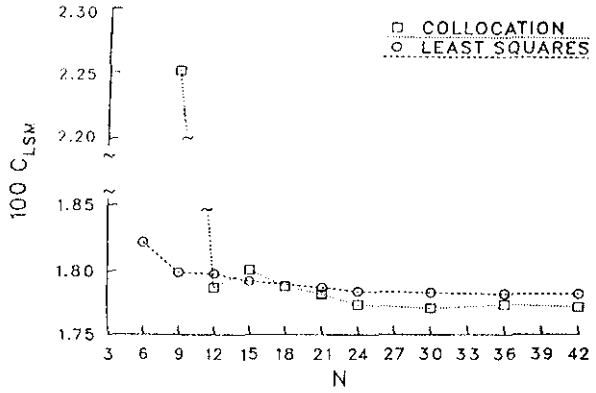

Fig. 3. Moment coefficient vs number of eigenvalues for Re = 21.5, f = 0.0621, and A = 1.042 calculated by LS and COL (note break in ordinate scale).

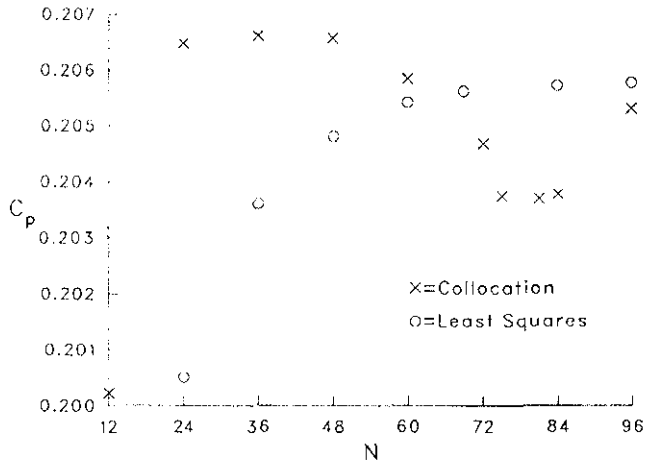

Fig. 4. Pressure coefficient at r = 0.667 vs number of eigenvalues for Re = 1000, f = 0.1, and A = 3.0 calculated by LS and COL.

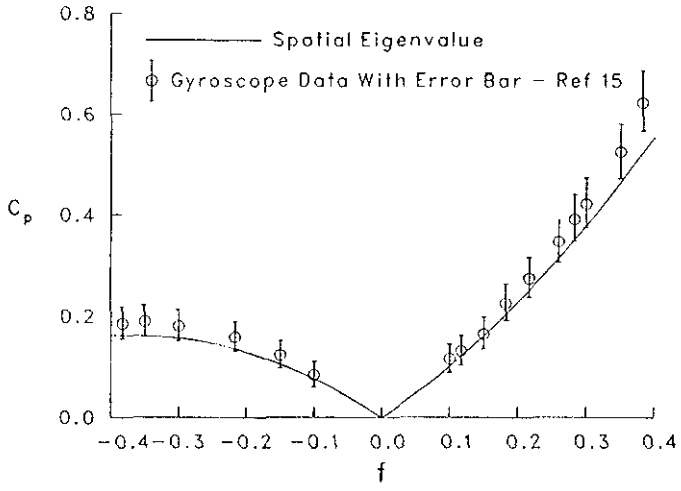

Fig. 5. Calculated pressure coefficient vs f compared with experimental measurements from Reference 4 for Re = 3.1, A = 3.148, and r = 0.667; for the experiment $K_0 = 2°$.

Estimates of errors in the measurements, from Reference 4, are included.

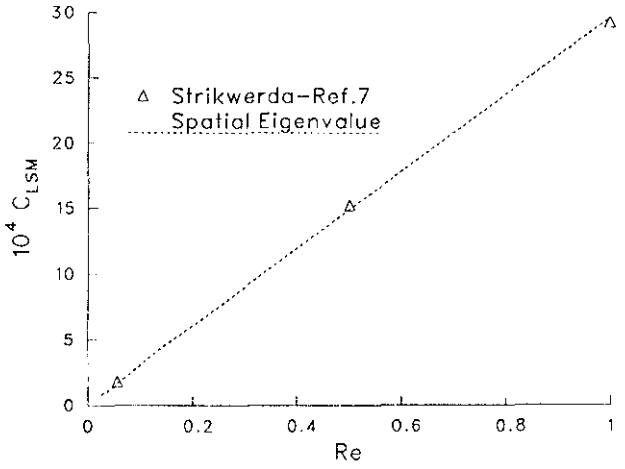

Fig. 6. Moment coefficient vs Re for f = 0.1, A = 3.0 according to the spatial eigenvalue method and Strikwerda's method, $K_0 = 2°$, $0 < Re \leq 1.0$.

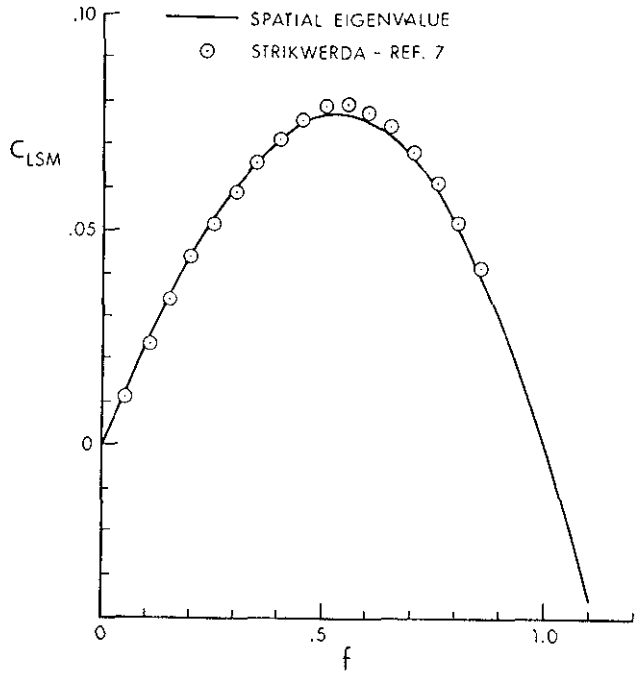

Fig. 7. Moment coefficient vs f for Re = 10, A = 3.0; $0 \leq f \leq 1.1$ for the spatial eigenvalue results and $.05 \leq f \leq 0.9$ and $K_0 = 2°$ for the Strikwerda results.

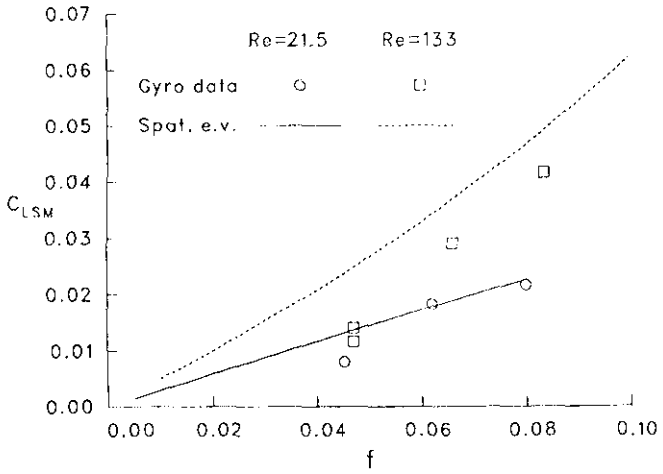

Fig. 8. Moment coefficient vs f for Re = 21.5, A = 1.042, and Re = 133.0, A = 1.486, according to spatial eigenvalue method and measurements from Reference 20 for K_0 = 2°.

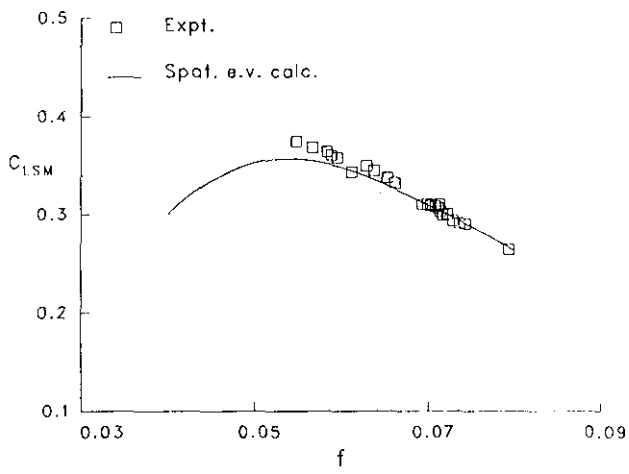

Fig. 9. Moment coefficient vs f for Re = 2415, A = 1.042 according to the spatial eigenvalue method and measurements of D'Amico (unpublished) with K_0 = 2°.